Optical properties of water-soluble L-cysteine-capped alloyed CdSeS quantum dot passivated with ZnSeTe and ZnSeTe/ZnS shells

Oluwasesan Adegoke[a], Tebello Nyokong[b], Patricia B.C. Forbes[a] *

[a]*Department of Chemistry, Faculty of Natural and Agricultural Sciences, University of Pretoria, Lynnwood Road, Pretoria 0002, South Africa*
[b]*Department of Chemistry, Rhodes University, Grahamstown 6140, South Africa*

Abstract

Alloyed quantum dots (QDs) passivated with shell materials have valuable optical characteristics suitable for a wide array of applications. In this work, alloyed ternary CdSeS QDs passivated with ZnSeTe and ZnSeTe/ZnS shells have been synthesized via a hot-injection method and a ligand exchange reaction employing L-cysteine as a thiol ligand has been used to obtain these water-soluble nanocrystals for the first time. The photoluminescence (PL) quantum yield (QY) of alloyed L-cysteine-capped CdSeS was 71.2% but decreased significantly to 5.2% upon passivation with a ZnSeTe shell. The red shift in PL emission of the CdSeS/ZnSeTe QDs was attributed to be strain-induced whilst a lattice-induced process likely created defect states in the core/shell interface hence contributing to the decline in the PL QY. Nonetheless, the fluorescence stability of CdSeS/ZnSeTe QDs in aqueous solution was unperturbed. Further passivation with a ZnS shell (CdSeS/ZnSeTe/ZnS) improved the PL QY to a value of 58.7% and thus indicates that the defect state in the QDs core/shell/shell structure was reduced. PL lifetime exciton measurements indicated that the rates of decay of the QDs influenced their photophysical properties.

Keywords: Quantum dots, core/shell, photoluminescence, quantum yield, alloy, hot-injection

*Corresponding author:
Email address: adegoke.sesan@mailbox.co.za (O. Adegoke), t.nyokong@ru.ac.za (T. Nyokong), patricia.forbes@up.ac.za (P.B.C. Forbes)

1. Introduction

The unique optical properties of semiconductor quantum dots (QDs) nanocrystals such as their broad absorption and narrow symmetric emission spectra, high surface-to-volume ratio, superior photostability and multiplex colour potentials **[1-4],** have stimulated their wide-spread applications in several facets of science and technology **[5-8].** Amongst the group II –VI classes of core QDs, CdTe and CdSe are the most popular but they often suffer from low photoluminescence (PL) quantum yields (QY) and reduced photostability. Passivation of the core with shell materials such as CdS **[9]** ZnSe **[10**] or ZnS **[11]** provides protection against surface traps hence the QY and photostability can be improved **[12].** In addition, other effects of shell passivation include red-shifting the PL emission of the nanocrystal to spectral ranges beyond the core **[13]**. This could be achieved depending on the type of shell materials, fabrication technique and lattice-induced strain between the core and shell material **[14].**

Recently, research attention has been directed to the synthesis of ternary alloyed QDs due to their size and composition-tunable bandgap **[15]**. Compared to binary core QDs, alloyed ternary core QDs have shown superior optical properties with reference to their improved photostability, QY and non-blinking emission properties. The various Cd-based ternary QDs that have been synthesized to date are

CdZnSe **[16,17**], CdZnTe **[18**], CdZnS **[19]**, CdSeTe **[20]** and CdSeS **[21].** In practice, controlling the synthesis of ternary QDs is however not trivial. There are two different methods that have been reported in literature by Zhong et al. **[22,23**]. The first is called the "embryonic nuclei-induced alloying process" **[22]** in which the first cationic precursors (either Zn or Cd) are injected into the solution to form the binary seeds and an increase in temperature is used to grow the ternary QDs by injection of the second cationic precursor. The second approach is called the "cationic exchange process" **[23]** and it involves firstly synthesizing the binary QDs (for example ZnSe) and the injection of a second cationic precursor (for example Cd^{2+}) produces the ternary nanocrystal. For the latter, a zinc blende crystal structure was reported **[23]** while the former produces a hexagonal crystal structure **[22].** Regardless of which of the two methods is adopted, a general requirement to obtain satisfactory optical properties is to ensure that both the core and shell materials crystallize in the same structure.

While most research has focused on studying the optical effects of passivation of shell layers on non-alloyed core QDs with low PL QY **[24-27],** little is known of the optical effects of passivation of shell layers on alloyed core QDs exhibiting high PL QY (>50%)**.** In our research group, our focus has been on studying the optical properties of shell materials overcoated on ternary alloyed QDs exhibiting high PL QY. Recently, passivation of shell layers on alloyed ternary CdSeS QDs has been of interest to us. In this work, we report for the first time on the deposition of alloyed ternary ZnSeTe and ZnSeTe/ZnS shells on CdSeS QDs exhibiting high PL QY. The binary seeds of CdSe QDs were synthesized first before forming the alloyed CdSeS

QDs. Fabrication of the QDs was performed via a one-pot approach and a ligand exchange reaction of the organic capping with L-cysteine thiol ligand produced water-soluble nanocrystals. In order to develop nanocrystals with mismatch alloys, alloyed ZnSeTe, represents an ideal candidate for such development due to the moderate mismatch between the anions (Se and Te) **[28]**. A mismatched alloy pair (such as Se and Te) is capable of producing nanocrystals with electronic changes in their structure, which results in density of states engineering [**29**] and abnormal bandgap bowing **[28].** The passivation of ZnS **[30]** and ZnO **[31]** shells on alloyed CdSeS has been documented in literature. However, this work is the first reported passivation of an alloyed ZnSeTe shell with a mismatch anion pair onto alloyed core QDs. We have harvested a single nanocrystal size of each of CdSeS, CdSeS/ZnSeTe and CdSeS/ZnSeTe/ZnS and studied their structural and optical properties.

2. Experimental Section

2.1. Materials

Trioctylphosphine oxide (TOPO), cadmium oxide, sulphur, zinc powder, 1-octadecene (ODE), tellurium powder, L-cysteine and oleic acid (OA) were purchased from Sigma Aldrich. Methanol, acetone, selenium powder and potassium hydroxide were purchased from Merck. Solutions of the QDs were prepared with ultra pure water obtained from a Milli-Q Water System.

2.2. Characterization

UV-vis absorption spectra were recorded on a Cary Eclipse (Varian) spectrophotometer. Fluorescence emission spectra were recorded on a Horiba Jobin Yvon Fluoromax-4 spectrofluorometer. Determination of the PL quantum yield (Φ_F) of the QDs was achieved by comparing the integrated fluorescence intensities of the QDs (*F*) in Millipore water to that of Rhodamine 6G (F_{Std} ; $\Phi_{F(Std)}$ = 0.95 **[32]**) in ethanol whilst taking into consideration the refractive indices (*n*) of the solvents and absorbance of each QD solution (*A*) and Rhodamine 6G (A_{Std}) at the excitation wavelength.

$$\Phi_F = \Phi_{F(Std)} \frac{F \,.\, A_{Std} \,.\, n^2}{F_{Std} \,.\, A \,.\, n_{Std}^2}$$

X-ray powder diffraction (XRD) patterns were analyzed using a PANalytical X'Pert Pro powder diffractometer in θ–θ configuration with an X'Celerator detector, variable divergence and receiving slits with Fe filtered Co-Kα radiation (λ=1.789Å). Transmission electron microscopy (TEM) images were obtained using a JEOL JEM 2100F operated at 200 kV. Fluorescence lifetime measurements were carried out using a time correlated single photon counting (TCSPC) setup (FluoTime 200, Picoquant GmbH). The excitation source was a diode laser (LDH-P-C-485 with 10 MHz repetition rate, 88 ps pulse width). Fluorescence was detected under the magic angle with a peltier cooled photomultiplier tube (PMT) (PMA-C 192-N-M, Picoquant) and integrated electronics (PicoHarp 300E, Picoquant GmbH). A monochromator with a spectral width of about 4 nm was used to select the required emission wavelength band. A scattering Ludox solution (DuPont) was used to measure the response function of the system and had a full width at half maximum (FWHM) of about 280 ps. To obtain good statistics, the ratio of stop to start pulses

was kept low (below 0.05). Measurement of the entire luminescence decay curve (range 0 to 100 ns) was at the maximum of the emission peak. Data analysis was performed using the Fluofit program (Picoquant GmbH).

2.3. Synthesis of the QDs

One-pot pyrolysis of hot-injection organometallic precursors was employed to fabricate the synthesis of alloyed CdSeS, CdSeS/ZnSeTe and CdSeS/ZnSeTe/ZnS QDs based on literature description but with modifications **[33].** Prior to the synthesis of the QDs, the required precursor solutions were firstly prepared as follows: a TOPSe solution containing Se and TOPO in ODE was prepared by dissolving 0.3 g of Se and 1.93 g of TOPO in 25 mL of ODE at 80 ^{o}C while the TOPTe solution was prepared by dissolving 0.48 g of Te and 1.93 g of TOPO in 25 mL of ODE at the same temperature. Zn and S precursors were prepared separately by dissolving 0.407 g of Zn powder and 0.16 g of S in 20 mL of OA and 30 mL of ODE.

The synthesis of the core QDs was carried out under Ar atmosphere at 280 ^{0}C by adding a portion of TOPSe precursor (10 mL) into a Cd-OA complex solution (1.3 g of CdO in 30 ml of OA and 50 mL of ODE) to form the CdSe binary seeds. Once satisfactory size of the CdSe QDs was obtained, the S precursor solution (10 mL) was injected into the growth solution to afford the nucleation and growth of the alloyed CdSeS QDs. Passivation of the alloyed CdSeS surface with ZnSeTe shell was carried out at a reduced temperature of 200 ^{0}C to prevent further growth of the CdSeS QDs. Zn (10 mL), TOPSe and TOPTe (each 5 mL) precursors were injected into the growth solution to overcoat the ZnSeTe shell around the alloyed core. Further passivation

with a ZnS shell was carried out at the same temperature by injection of 5 mL each of Zn and S precursors. The QDs were purified with methanol and acetone.

2.4. Water-solubilization with L-cysteine

Hydrophilic portions of the QDs were obtained by a ligand exchange reaction involving a KOH-methanolic-L-cysteine-H_2O solution to replace the organic capping of the QDs with L-cysteine thiol ligand. The KOH-methanolic-L-cysteine solution was firstly prepared by dissolving 3.0 g of KOH in 40 mL of methanol and 2.0 g of L-cysteine was added and dissolved ultrasonically. The ligand exchange reaction was carried out by dissolving each of the QDs in chloroform and adding the QDs solution to separate portions of the KOH-methanolic-L-cysteine solution. An appropriate volume of water (20 mL) was additionally added. The water-soluble QDs thus obtained were purified and centrifuged repeatedly with acetone and chloroform. Further purification was carried out using a H_2O:chloroform:acetone (1:1:2) mixture to remove all unreacted organic constituents. The purified QDs were dried in a fume hood.

3. Results and discussion

3.1. Fabrication and purification strategy

Scheme 1 shows the one-pot organometallic hot-injection synthetic route and ligand exchange reaction employed in the fabrication of the QDs. The molar composition of Se, Te, Zn and S were maintained throughout the synthetic process. The nucleation and subsequent growth of CdSe during the initial mixing of TOPSe into the Cd-OA solution was rapid and this was reflected by the sudden change in the colour of the

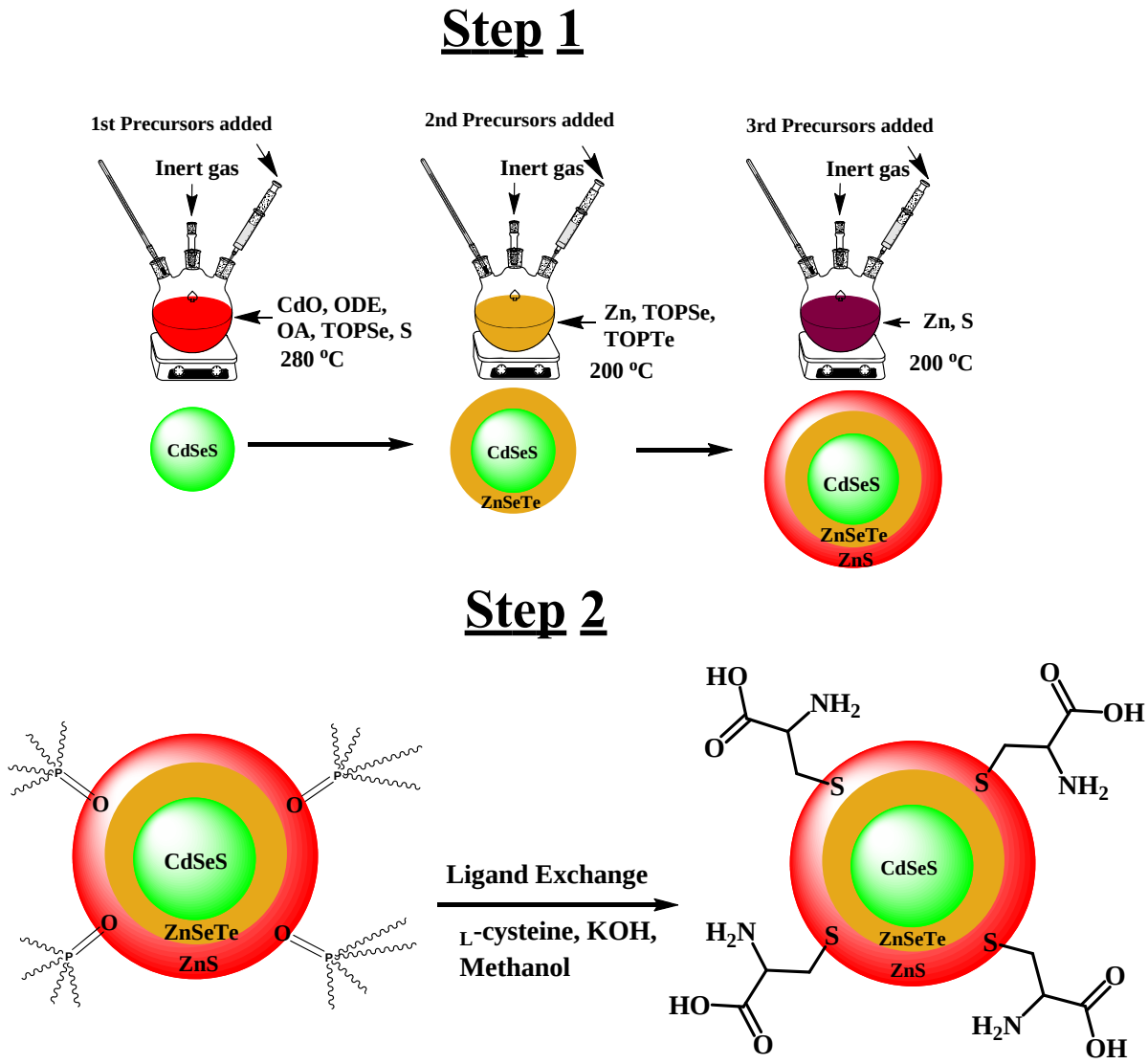

Scheme 1. Schematic representation of the synthesis and ligand exchange reaction of the QD nanocrystals. CdSeS/ZnSeTe/ZnS QDs are used as an example for the ligand exchange reactions of the QDs.

reaction mixture from colourless to red within 3 s of injection of TOPSe precursor, and it then turned rapidly deeper red to indicate the growth of the CdSe core. The initial rapid growth was followed by a slow growth phase of the nanocrystal. Preliminary investigations showed that it was more appropriate to add the Se precursor before the S precursor, as we found that TOPSe was more reactive to the Cd-OA solution than S. Hence, based on our synthetic approach, CdSe binary QDs were formed before forming the alloyed CdSeS QDs.

Overgrowth of alloyed ternary ZnSeTe and alloyed ternary/binary ZnSeTe/ZnS shells was carried out at a reduced temperature of 200 ^{o}C to prevent further growth of the alloyed CdSeS core. During the shelling process, the QDs grew slower than the alloyed core. The slow growth is mainly explained by the process called Oswald ripening in which smaller particles dissolved to produce larger particles **[34]**.

The QDs were passed through a rigorous process of purification as follows: (a) precipitate in acetone, centrifuge repeatedly and decant supernatant → purification step 1. (b) re-disperse in chloroform, centrifuge repeatedly and decant supernatant → purification step 2. (c) re-disperse in H_2O:chloroform:acetone (1:1:2), centrifuge repeatedly and decant supernatant → purification step 3. (d) re-disperse in chloroform or acetone, centrifuge repeatedly and decant supernatant → purification step 4.

3.1. Structural properties

TEM micrographs and the corresponding histograms of the particle size distribution of the water-soluble L-cysteine-capped alloyed CdSeS core, CdSeS/ZnSeTe

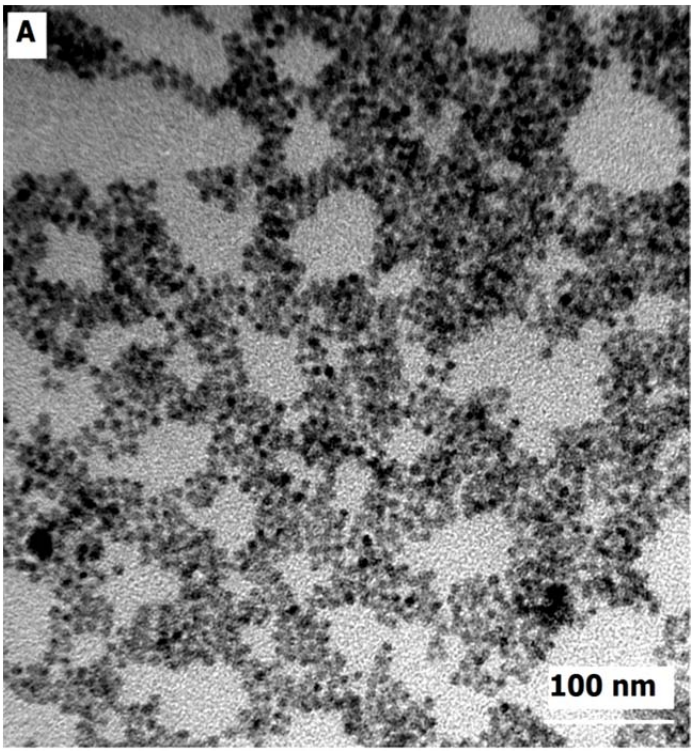
A
100 nm

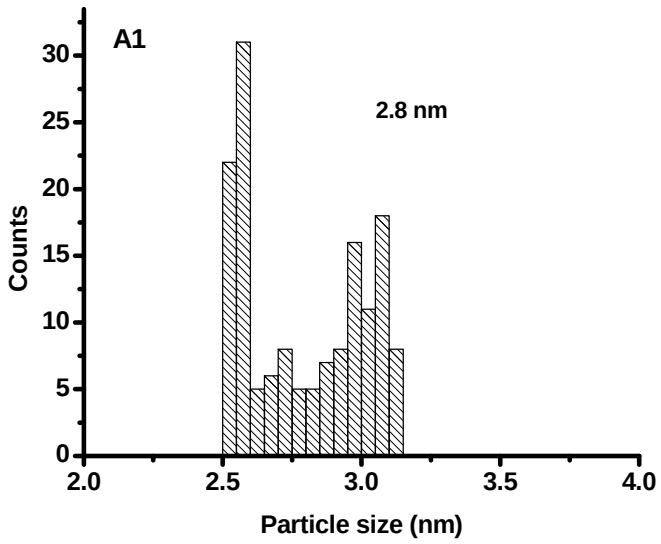
A1
2.8 nm
Counts
0
5
10
15
20
25
30
2.0
2.5
3.0
3.5
4.0
Particle size (nm)

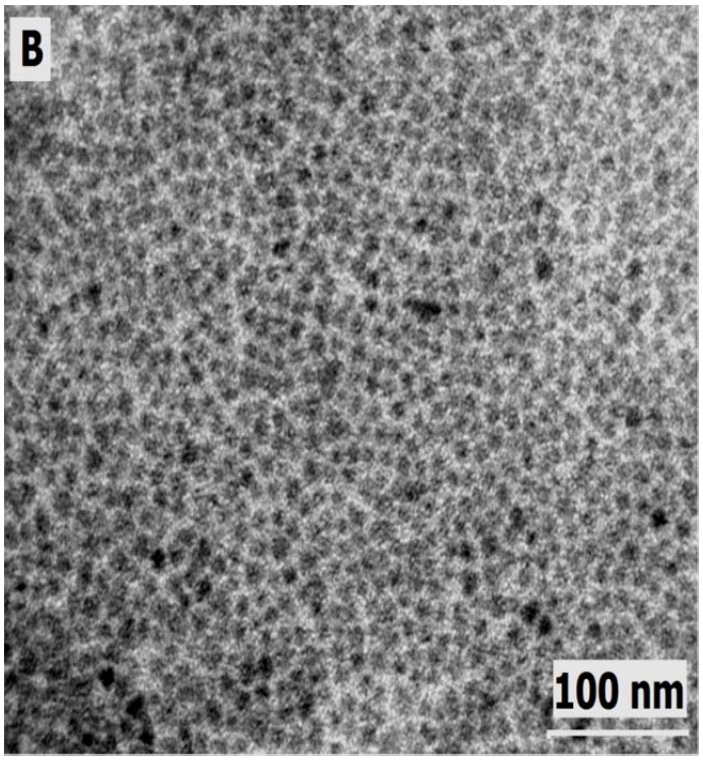
B
100 nm

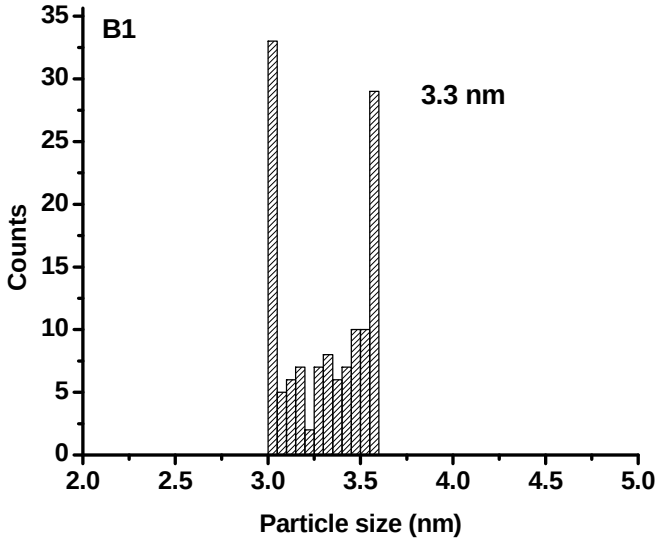
B1
3.3 nm
Counts
Particle size (nm)
0
5
10
15
20
25
30
35
2.0
2.5
3.0
3.5
4.0
4.5
5.0

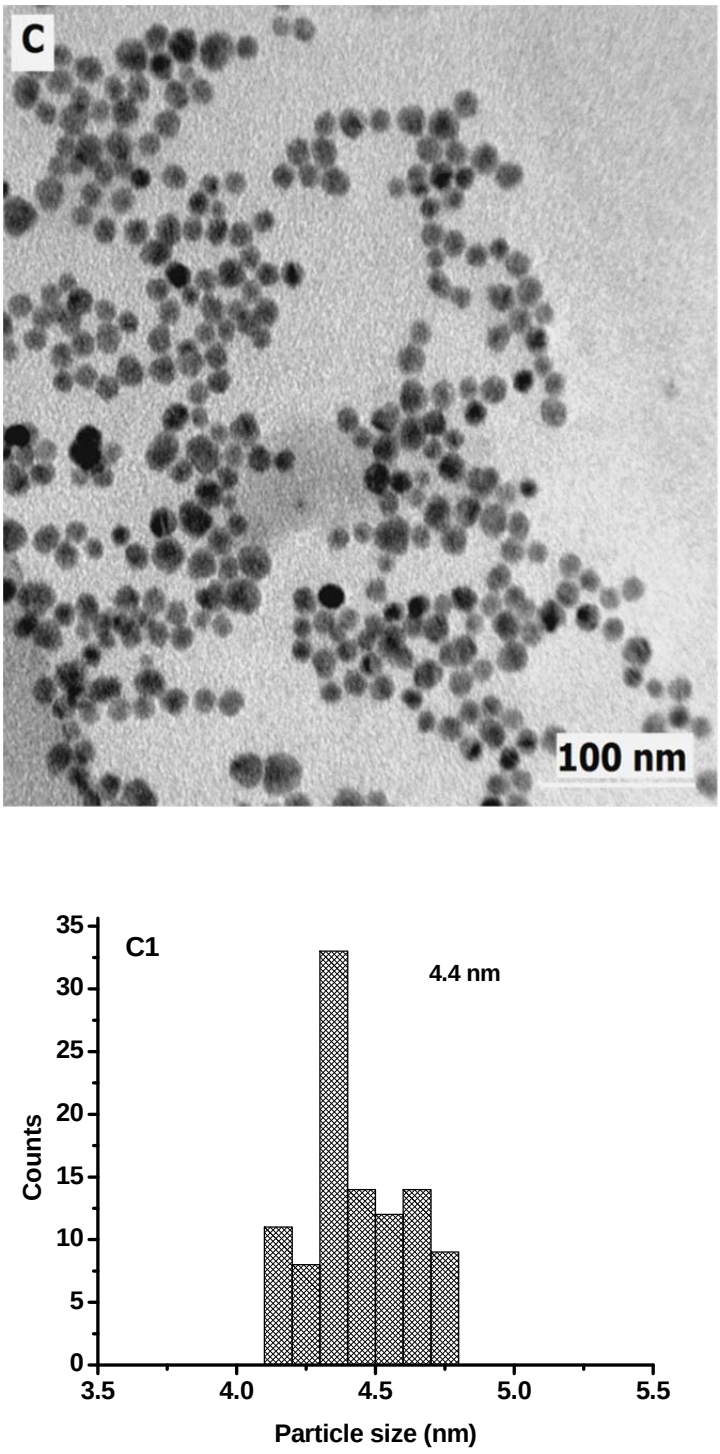

Fig. 1. TEM images of alloyed L-cysteine-capped (A) CdSeS, (B) CdSeS/ZnSeTe and (C) CdSeS/ZnSeTe/ZnS QDs. Corresponding histograms showing the particle size distribution of the QDs are denoted as A1, B1 and C1.

core/shell and CdSeS/ZnSeTe/ZnS core/shell/shell QDs are shown in Fig. 1. The particle size distribution for CdSeS QDs are nearly monodispersed and spherical in shape. Upon formation of CdSeS/ZnSeTe QDs, irregularity in the shape of the particle distribution was observed but the monodispersity of the particles was improved relative to the core CdSeS. The TEM image of CdSeS/ZnSeTe/ZnS QDs revealed a distinct spherical shape pattern of the particle distribution and also showed that the particles were homogenous and highly monodispersed. The information inferred from the TEM images provides direct evidence that the overcoating of ZnSeTe and of ZnSeTe/ZnS shells on alloyed CdSeS QDs altered the monodispersity of the particles and indicates morphological changes in the QD structure. The average size distribution of the QDs measured were 2.8 nm for CdSeS, 3.3 nm for CdSeS/ZnSeTe and 4.4 nm for CdSeS/ZnSeTe/ZnS. The increase in the particle size distribution of the QDs upon shell deposition demonstrates that the QDs exhibit the quantum size effect phenomenon **[35]**.

The powder XRD pattern of the QDs shown in Fig. 2 reveal a lack of phase change upon deposition of the shell layers which implies that the crystallinity of the QDs was preserved upon passivation with ZnSeTe and ZnSeTe/ZnS shells. The diffraction pattern of the QDs corresponds to the typical zinc-blende crystal structure with planes at {111}, {200} and {311}. The observation of a slight shift to higher Bragg angle in the peak position of alloyed CdSeS relative to the CdSe core confirms the formation of the alloyed core nanocrystal. This slight shift in peak position provides concrete evidence that the structure of the core QDs was modified and hence that the alloyed nanocrystal was formed. Comparing the peak positions of

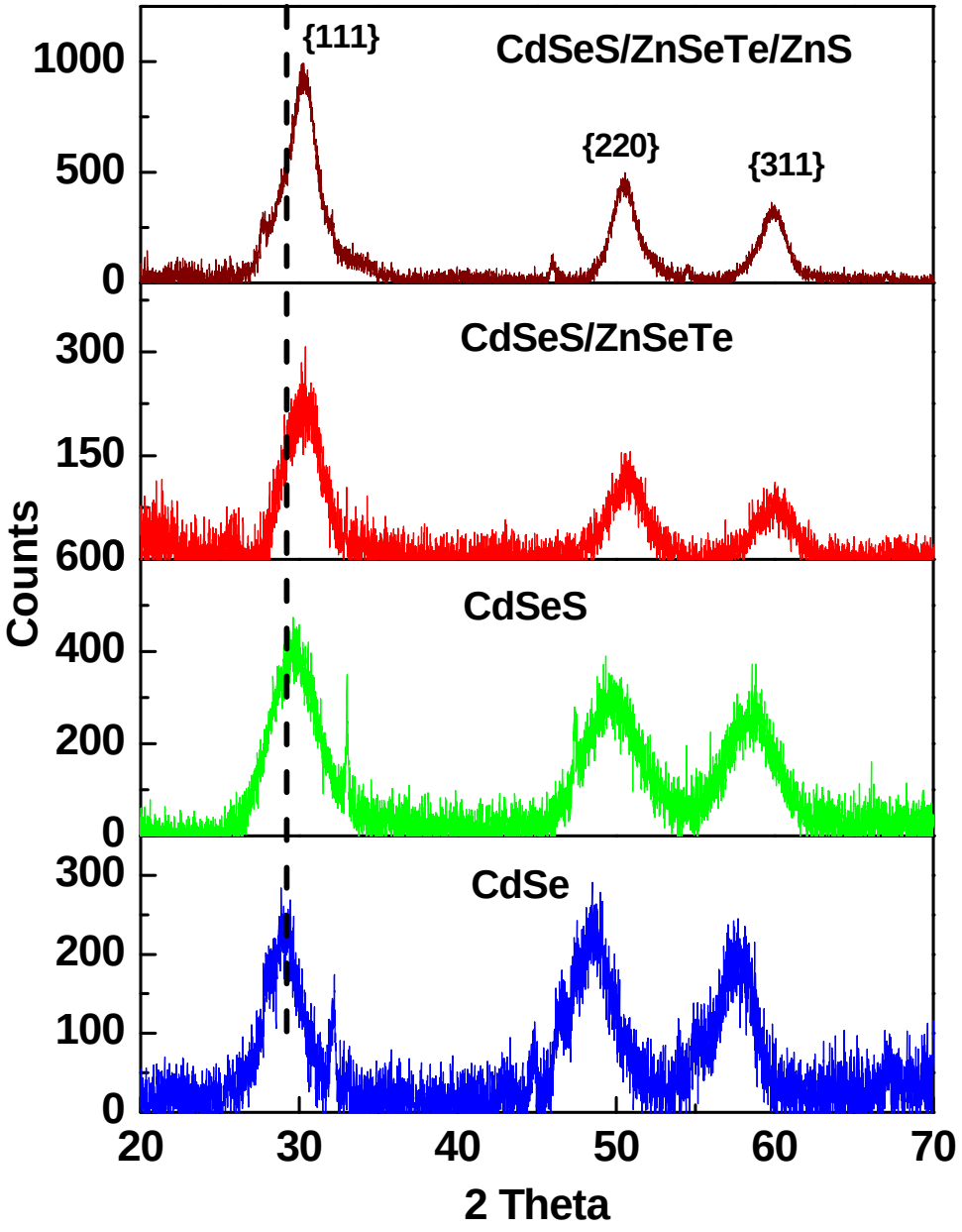

Fig. 2. Powder XRD patterns for L-cysteine-capped CdSe, CdSeS, CdSeS/ZnSeTe and CdSeS/ZnSeTe/ZnS QDs.

CdSeS/ZnSeTe to that of CdSeS, it is clearly evident that the diffraction peaks of CdSeS/ZnSeTe also shifted slightly to a higher Bragg angle and hence confirms the formation of the core/shell structure. Formation of CdSeS/ZnSeTe/ZnS QDs did not induce any noticeable shift in the diffraction peak. It is important to note that such a lack of peak shift upon passivation with a ZnS shell has also been reported in the literature for a ZnS passivated CdTe/CdSe surface **[11]**.

3.2. Optical properties

Fig. 3 shows the room temperature absorption and PL emission spectra of the L-cysteine-capped CdSe, alloyed CdSeS, CdSeS/ZnSeTe and CdSeS/ZnSeTe/ZnS QDs measured in Millipore water. It is clearly evident that the absorption spectra of the QDs do not possess the same spectral features with reference to the presence of the excitonic peaks. However, the PL spectra each revealed a single narrow Gaussian-shaped peak with the full width and half maximum (FWHM) within the range of 35-42 nm (Table 1). For the core CdSe QDs, two distinct excitonic peaks were observed which indicated a band edge type of absorption feature. A similarity with respect to the absorption spectrum of CdSe QDs was observed for the alloyed CdSeS QDs. The only difference between the excitonic peaks of CdSe and CdSeS is that for the later, the excitonic peak in the high energy region is broadened in comparison to CdSe. Further broadening of the peaks in the absorption spectra of the QDs upon shell deposition was observed with evidence of complete disappearance of the excitonic peaks in the lower and higher-wavelength position for CdSeS/ZnSeTe/ZnS QDs

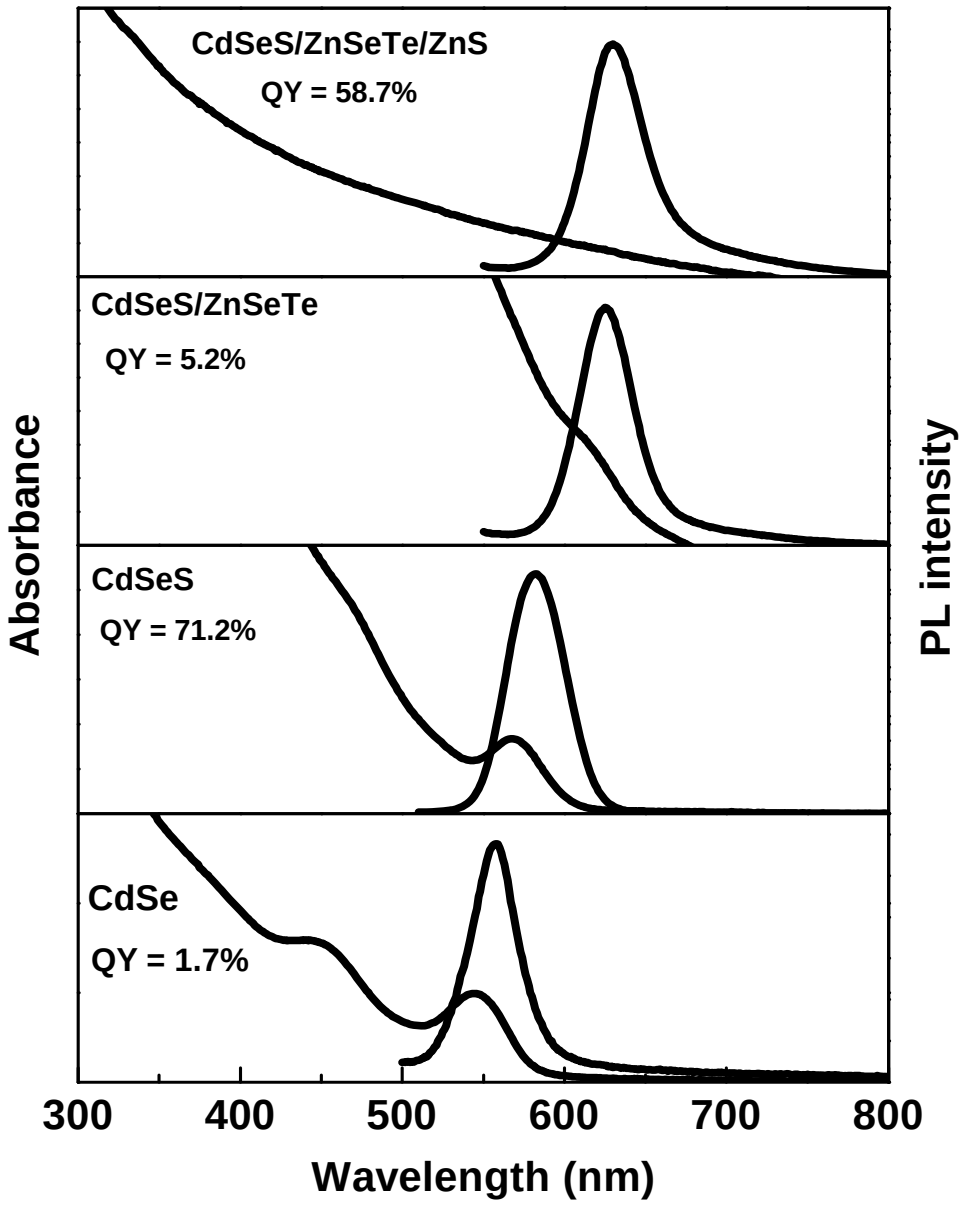

Fig. 3. Absorption and PL emission spectra of L-cysteine-capped CdSe, alloyed CdSeS, CdSeS/ZnSeTe and CdSeS/ZnSeTe/ZnS QDs. λ_{exc} = 500 nm.

Table 1. Photophysical parameters for L-cysteine-capped CdSe, alloyed CdSeS, CdSeS/ZnSeTe and CdSeS/ZnSeTe/ZnS QDs.

QDs	**λ_{emi} (nm)**	**QY (%)**	**FWHM (nm)**	**τ_1 (ns)[a]**	**τ_2 (ns)[a]**	**τ_3 (ns)[a]**	**τ_{av}[b] (ns)**
CdSe	558	1.7	35	8.2(0.14)	2.2(0.63)	0.7(0.23)	2.70
CdSeS	582	71.2	41	11.2(0.25)	3.4(0.53)	0.8(0.22)	4.78
CdSeS/ZnSeTe	625	5.2	38	9.5(0.17)	0.5(0.39)	2.2(0.44)	2.84
CdSeS/ZnSeTe/ZnS	630	58.7	42	17.6(0.38)	2.6(0.42)	0.7(0.20)	7.92

[a]Relative abundance in brackets, [b]average lifetime

(Fig. 3). The broadening of the excitonic peaks could be due to increased delocalization of the exciton in the core as the shell layers were formed **[36]**.

Formation of alloyed CdSeS, CdSeS/ZnSeTe and CdSeS/ZnSeTe/ZnS induced a red-shift of the PL emission wavelength of the QDs (Fig. 3 and Table 1). The absorption spectra of the QDs also red-shifted but broadened as the shell layers were deposited as discussed above. The broadening of the absorption spectra is typical of alloyed QDs formation as demonstrated in the literature **[37]**. CdSe core QDs were harvested at a PL emission wavelength of 558 nm and a red-shift of 24 nm was observed when the alloyed CdSeS QDs were harvested at 582 nm. Formation of CdSeS/ZnSeTe also induced a considerable red-shift of the emission wavelength by 43 nm relative to the alloyed core while a 5 nm emission red-shift was observed for CdSeS/ZnSeTe/ZnS relative to CdSeS/ZnSeTe. A very low PL QY yield of 1.7% was measured for CdSe whilst the QY value for alloyed CdSeS QDs increased dramatically to 71.2%. This confirms that the optical properties of alloyed core QDs are far superior to those of conventional CdSe QDs. Also, it is important to note that the QY value for alloyed CdSeS QDs is indeed remarkable, considering that the water-dispersible QDs were produced via ligand exchange reaction which is known to reduce or lead to total loss of fluorescence. It is difficult to compare the QY of our alloyed CdSeS QDs with those reported in the literature since this is the first reported water-soluble CdSeS QDs obtained via ligand exchange reaction. In addition, the high PL QY of CdSeS QDs is an indication of a low defect state and relatively slow radiationless recombination rates. The low defect state could be

attributed to a combination of an effective surface passivation, reconstruction and relaxation as well as a slow heteroepitaxial growth and reaction conditions **[38,39].**

Formation of CdSeS/ZnSeTe core/shell decreased the PL QY significantly to 5.2% which implies that surface defects led to the creation of nonradiative recombination in the core/shell interface. The significant decline in the QY of the core/shell QDs may also be due to the anisotropic shell growth with reference to the TEM image (Fig. 1B) which indicates that the shape of the nanoparticle was highly heterogenous. The shell growth may have induced strain or dislocation at the CdSeS→ZnSeTe heterointerface. In addition, the mismatch Se and Te pair in the ZnSeTe layer could also play a role in creating defect states in the core/shell structure. Hence, we can attribute the red-shift in PL emission of CdSeS/ZnSeTe to be a strain-induced shift **[14]**. For applications such as biomechanics and optoelectronics, the effect of strain on materials is of fundamental importance **[14]**. Studies have shown that based on the complex relationship between strain and nanomaterials, novel nanostructures with unique properties can be produced through lattice strain **[40,41].**

To further understand the mechanism of strain tuning, we have employed the theory of Smith et al **[14]** to critically probe our core/shell system. We hypothesize that rather than the core/shell QDs forming a concentric sphere, the nonspherical shape of the QDs revealed via TEM analysis indicate that a concentric cylinder was formed **[14]**. We further hypothesize that as the ZnSeTe shell was coated around the alloyed core, the strain energy may have been equal to the energy required to induce a lattice mismatch defect. Hence, the optical properties of the core/shell QDs favoured both a strained-induced formation and a lattice-induced defect.

Overcoating of an additional ZnS shell layer around the alloyed CdSeS/ZnSeTe surface improved the PL QY dramatically to a value of 58.7 %. The sharp increase in the QY for CdSeS/ZnSeS/ZnS QDs is quite intriguing and provides direct evidence that the surface of CdSeS/ZnSeTe was well passivated with the ZnS shell, hence the defect states were minimized. The homogenous display of the particle size distribution of the QDs as evident from TEM analysis (Fig. 1C) also confirms the passivating effect of the ZnS shell. In addition, despite the broadening and disappearance of the excitonic absorption peaks in CdSeS/ZnSeTe/ZnS QDs, the FWHM of the PL emission peak was still relatively narrow which implies that the CdSeS/ZnSeTe/ZnS QDs may have sandwiched between an indirect exciton and direct exciton.

Lattice constants for a range of the nanocrystals have been reported in literature; 5.95 for CdSeS **[42]**, 5.8 for ZnSeTe **[28]** and 3.82 Å for ZnS **[43].** It is important to note that the lattice constants for CdSeS and ZnSeTe depend on the fractional composition with respect to S for the former and Te for the later, and values relating to a 0.5 fraction were reported here. The estimated lattice mismatch between CdSeS and ZnSeTe is 2.6% while that for CdSeS and ZnS is 35.8%. It is interesting to note that the passivation of the core with a ZnSeTe shell induced a significant decrease in the PL QY despite the small lattice mismatch while conversely, the large lattice mismatch observed between CdSeS and ZnS significantly improved the PL QY of the resultant core/shell/shell QDs. These results demonstrate that the optical properties of alloyed QDs are indeed different from those of conventional non-alloyed QDs.

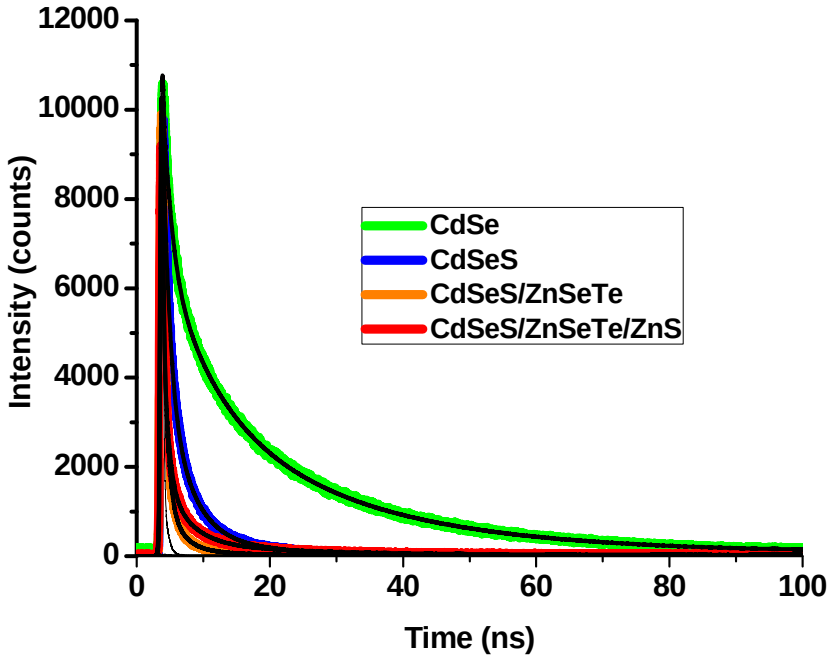

Fig. 4. Time-resolved PL spectra of L-cysteine-capped CdSe, CdSeS, CdSeS/ZnSeTe and CdSeS/ZnSeTe/ZnS QDs.

To further understand the optical behaviour of the QDs, we have employed time-resolved PL lifetime measurements to probe the exciton dynamics. The PL decay curves of the alloyed CdSeS, CdSeS/ZnSeTe and CdSeS/ZnSeTe/ZnS QDs are shown in Fig. 4. We have successfully simulated the PL lifetimes of the QDs in a triexponnential decay manner and the averages of these lifetimes have been used as a basis for interpretation (Table 1). The longer lifetime τ_1, is attributed to surface state effects in the carrier recombination process **[44]**, while the intermediate lifetime τ_2 arises from intrinsic recombination processes of initially populated core states **[45]** and the shortest lifetime τ_3 is likely due to radiative depopulation from band edge recombination at the surface **[45]**. From the longer lifetime data, it could be seen that the CdSe core QDs which exhibited a very low PL QY of 1.7% decayed faster than the rest of the QDs whilst alloyed CdSeS QDs with a high PL QY of 71.2% decayed much slower than CdSe which indicates that effective radiative recombination exciton rates favour a slower decay. Also, the longer lifetime for CdSeS/ZnSeTe/ZnS decayed much slower than CdSeS/ZnSeTe, hence demonstrating the passivating effect of the ZnS layer as observed from the differences in their PL QY. For the intermediate lifetime values, the trend was the same as those of the longer lifetimes when taking into consideration the rates of decay. For the shortest lifetimes, the trend was not the same with the longer and intermediate lifetimes, hence the average lifetimes of the QDs have been calculated to provide a clearer picture of the decay rates (Table 1).

3.3. Stability of the QDs.

The stability of QDs is one of the essential parameters used to judge their quality. For biological and chemical applications requiring the continuous or prolonged output of photons, it is important that the QD nanocrystals are stable. High stability of QDs can eliminate OFF/ON fluorescent blinking problems associated with most QDs system and it can also prevent false positive data in fluorescence signals for sensing/biosensing applications. Hence we carried out a preliminary investigation of the stability of the QDs in aqueous solution by exposing them to ambient light for 21 days. If the QDs are unstable, they should precipitate out from solution and this will be reflected in the quenching of their PL intensity. To ensure the alloyed CdSeS core QDs do possess higher stability than the conventional CdSe QDs, we have compared their fluorescence stability.

Fig. 5 shows the fluorescence spectra of the QDs measure before and after 21 days of exposure to ambient light. It is clearly evident that after 21 days, the fluorescence of CdSe QDs was quenched while that of alloyed CdSeS QDs was enhanced. This provides direct evidence that alloyed CdSeS QDs exhibits higher fluorescence stability than the conventional CdSe QDs. PL enhancement was also observed for the CdSeS/ZnSeTe core/shell and CdSeS/ZnSeTe/ZnS core/shell/shell QDs after 21 days of measurement. This implies that alloyed CdSeS, CdSeS/ZnSeTe and CdSeS/ZnSeTe/ZnS QDs will be suitable fluorophores in a wide variety of chemical and biological applications requiring prolonged downshifting of light. It is important to note that further investigation of the photostability of the QDs involving exposure to a higher energy light source (such as that provided by a laser) is needed to fully demonstrate the photostability of these QDs.

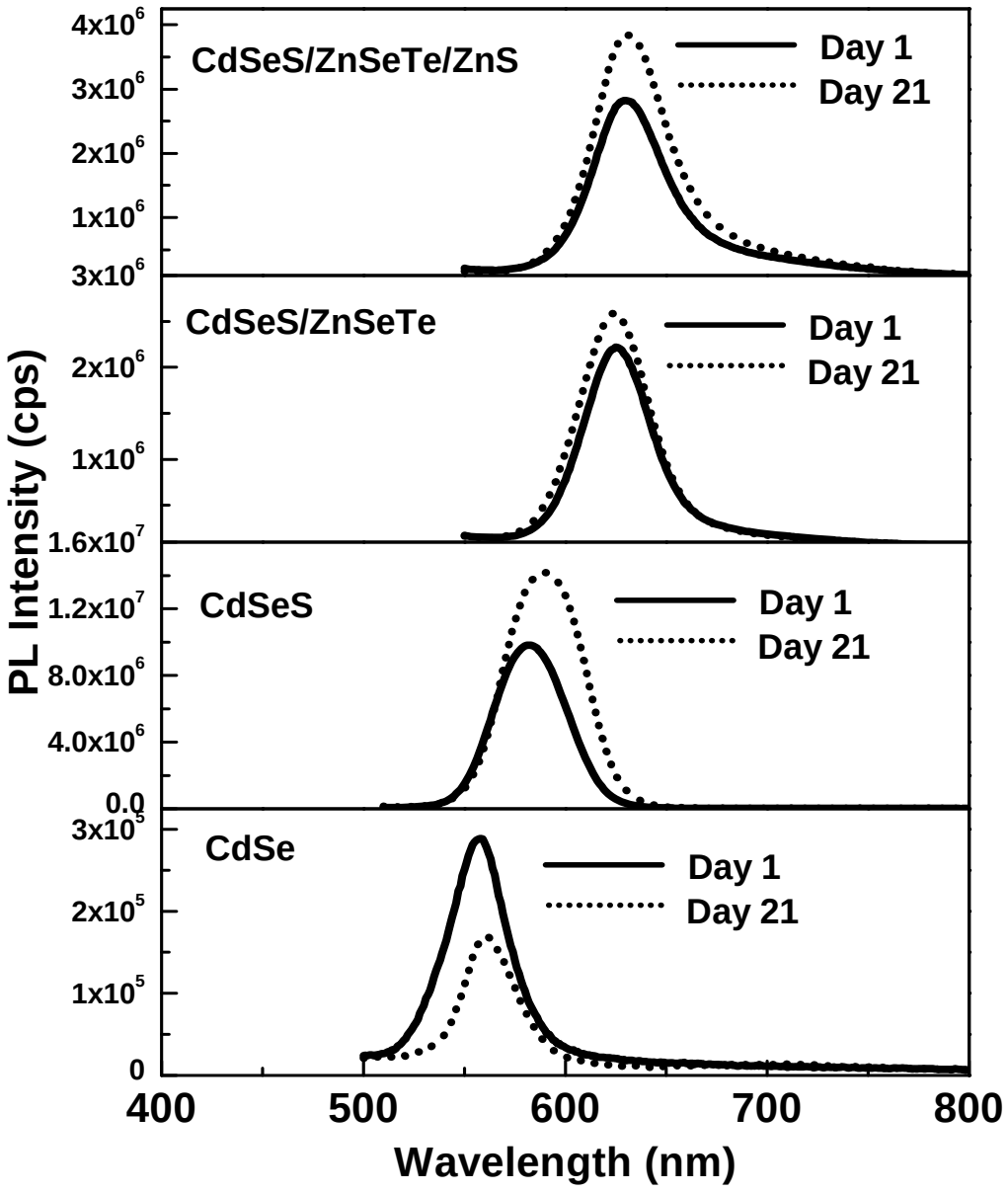

Fig. 5. PL stability of the QDs measured before (solid line) and after 21 days (dotted line) of exposure to ambient light.

4. Conclusion

In summary, we have successfully synthesized water-soluble L-cysteine-capped alloyed ternary CdSeS QDs exhibiting high PL QY. Passivation with ZnSeTe and ZnSeTe/ZnS shells produced optical information suitable for a wide array of applications. The superior optical properties of CdSeS QDs over conventional CdSe QDs were confirmed. Passivation of CdSeS with a ZnSeTe shell (CdSeS/ZnSeTe) decreased the PL QY but did not affect the PL stability. Defect states created in the core/shell interface was attributed to the decline in the PL QY. Conversely, the defect state was minimized upon passivation with a ZnS shell. PL lifetime exciton measurements provided valuable information about the rates of decay of the QDs and its influence on their photophysical properties.

Acknowledgements

A postdoctoral fellowship offered by the University of Pretoria is gratefully appreciated by O. Adegoke. This work is based on research supported in part by the National Research Foundation of South Africa, Grant Numbers: 92584, 90720 and 93394 (P. Forbes). Wirsam Scientific, South Africa is thanked for their support of this research. We thank the Electron Microscopy Unit, University of Pretoria (UP), for assistance with the TEM measurements and Wiebke Grote of UP for the XRD measurements.

References

1. R.C. Somers, M.G. Bawendi, D.G. Nocera, CdSe nanocrystal based chem-/ bio-sensors. Chem. Soc. Rev. 36 (2007) 579–591.
2. N. Tessler, V. Medvedev, M. Kazes, S.H. Kan, U. Banin, Efficient near-infrared polymer nanocrystal light-emitting diodes. Science 295 (2002) 1506–1508.
3. L. Peng, Y. Wang, Q. Dong, Z. Wang, Passivated ZnSe nanocrystals prepared by hydrothermal methods and their optical properties. Nano-Micro. Lett. 2 (2010) 190–196.
4. J. Wu, Z.M. Wang, V.G. Dorogan, S. Li, Y.I. Mazur, J.G. Salamo, Nanoscale, near infrared broadband emission of $In_{0.35}Ga_{0.65}As$ quantum dots on high index GaAs surfaces. Nanoscale 3 (2011) 1485–1488.
5. I.L. Medintz, H.T. Uyeda, E.R. Goldman, H. Mattoussi, Quantum dot bioconjugates for imaging, labelling and sensing. Nat. Mater. 4 (2005) 435–446.
6. O. Chen, J. Zhao, V.P. Chauhan, J. Cui, C. Wong, D.K. Harris, H. Wei, H.-S. Han, D. Fukumura, R.K. Jain, M.G. Bawendi, Compact high-quality CdSe-CdS core-shell nanocrystals with narrow emission linewidths and suppressed blinking. Nat. Mater. 12 (2013) 445–451.
7. K. Zhang, Q. Mei, G. Guan, B. Liu, S. Wang, Z. Zhang, Ligand replacement-induced fluorescence switch of quantum dots for ultrasensitive detection of organophosphorothioate pesticides. Anal. Chem. 82 (2010) 9579–9586.
8. T.K.C. Tran, D.C. Vu, T.D.T. Ung, H.Y. Nguyen, N.H. Nguyen, T.C. Dao, T.N. Pham, Q.L. Nguyen, Fabrication of fluorescence-based biosensors from

functionalized CdSe and CdTe quantum dots for pesticide detection. Adv. Nat. Sci.: Nanosci. Nanotechnol. 3 (2012) 035008.

9. X. Peng, M.C. Schlamp, A.V. Kadavanich, A. Alivisatos, Epitaxial Growth of Highly Luminescent CdSe/CdS Core/Shell Nanocrystals with Photostability and Electronic Accessibility. J. Am. Chem. Soc. 119 (1997) 7019−7029.
10. D.V. Talapin, I. Mekis, S. Götzinger, A. Kornowski, O. Benson, H. Weller, CdSe/CdS/ZnS and CdSe/ZnSe/ZnS Core-Shell-Shell Nanocrystals. J. Phys. Chem. B 108 (2004) 18826-18831.
11. W. Zhang, G. Chen, J. Wang, B.-C. Ye, X. Zhong, Design and Synthesis of Highly Luminescent Near-Infrared-Emitting Water-Soluble CdTe/CdSe/ZnS Core/Shell/Shell Quantum Dots. Inorg. Chem. 48 (2009) 9723-9731.
12. X. Brokmann, L. Coolen, M. Dahan, J.P. Hermier, Measurement of the Radiative and Nonradiative Decay Rates of Single CdSe Nanocrystals through a Controlled Modification of their Spontaneous Emission. Phys. Rev. Lett. 93 (2004) 107403-1-107403-4.
13. C.-Y. Chen, C.-T. Cheng, C.-W. Lai, Y.-H. Hu, P.-T. Chou, Y.-H. Chou, H.-T. Chiu, Type-II CdSe/CdTe/ZnTe (Core–Shell–Shell) Quantum Dots with Cascade Band Edges: The Separation of Electron (at CdSe) and Hole (at ZnTe) by the CdTe Layer. Small 1 (2005) 1215-1220.
14. A.M. Smith, A.A. Mohs, S. Nie, Tuning the Optical and Electronic Properties of Colloidal Nanocrystals by Lattice Strain. Nat. Nanotechnology 4 (2009) 56-63.
15. B.C. Fitzmorris, Y.-C. Pu, J.K. Cooper, Y.-F. Lin, Y.-J. Hsu, Y. Li, J.Z. Zhang, Optical Properties and Exciton Dynamics of Alloyed Core/Shell/Shell

$Cd_{1-x}Zn_xSe$/ZnSe/ZnS Quantum Dots. Appl. Mater. Interfaces 5 (2013) 2893-2900.

16. Y. Sheng, J. Wei, B. Liu, L. Peng, A facile route to synthesize CdZnSe core–shell-like alloyed quantum dots via cation exchange reaction in aqueous system. Mater. Res. Bull. 57 (2014) 67-71.
17. Y.G. Zheng, Z.C. Yang, J.Y. Ying, Aqueous Synthesis of Glutathione-Capped ZnSe and Zn1–xCdxSe Alloyed Quantum Dots. Adv. Mater. 19 (2007) 1475–1479.
18. J.Y. Ouyang, C.I. Ratcliffe, D. Kingston, B. Wilkinson, J. Kuijper, X.H. Wu, J.A. Ripmeester, K. Yu, Gradiently alloyed $Zn_xCd_{1-x}S$ colloidal photoluminescent quantum dots synthesized via a noninjection one-pot approach. J. Phys. Chem. C 112 (2008) 4908–4919.
19. W.K. Bae, M.K. Nam, K. Char, S. Lee, Gram-Scale One-Pot Synthesis of Highly Luminescent Blue Emitting Cd1− x Zn x S/ZnS Nanocrystals. Chem. Mater. 20 (2008) 5307-5313.
20. R.E. Bailey, S.M. Nie, Alloyed Semiconductor Quantum Dots: Tuning the Optical Properties without Changing the Particle Size. J. Am. Chem. Soc. 125 (2003) 7100-7106.
21. B. Wang, Y. Jiang, C. Liu, X. Lan, X. Liu, W. Wang, H. Duan, Y. Zhang, S. Li, Z. Zhang, One-pot synthesis of homogeneous $CdSe_xS_{1-x}$ alloyed quantum dots with tunable composition in a green N-oleoylmorpholine solvent. Phys. Status Solidi A 209 (2012) 306-312.
22. X.H. Zhong, Z.H. Zhang, S.H. Liu, M.Y. Han, W. Knoll, J. Phys. Chem. B 108 (2004) 15552–15559.

23. X.H. Zhong, Y.Y. Feng, Y.L. Zhang, Z.Y. Gu, L. Zou, Embryonic Nuclei-Induced Alloying Process for the Reproducible Synthesis of Blue-Emitting $Zn_xCd_{1-x}Se$ Nanocrystals with Long-Time Thermal Stability in Size Distribution and Emission Wavelength. Nanotechnology 18 (2007) 385606–385611.
24. A. Samanta, Z. Deng, Y. Liu, Aqueous Synthesis of Glutathione-Capped CdTe/CdS/ZnS and CdTe/CdSe/ZnS Core/Shell/Shell Nanocrystal Heterostructures. Langmuir 28 (2012) 8205-8215.
25. J. Yang, Q. Ma, P. Yang, Tunable luminescence of spherical CdSe/ZnS and tetrahedron $CdSe/Cd_{1-x}Zn_xS$ core/shell quantum dots created using same cores. Mater. Chem. Phys. 135 (2012) 486-492.
26. H. Seo, S.-W. Kim, In Situ Synthesis of CdTe/CdSe Core-Shell Quantum Dots. Chem. Mater. 19 (2007) 2715-2717.
27. I. Mekis, D.V. Talapin, A. Kornowski, M. Haase, H. Weller, One-Pot Synthesis of Highly Luminescent CdSe/CdS Core-Shell Nanocrystals via Organometallic and "Greener" Chemical Approaches. J. Phys. Chem. B 107 (2003) 7454-7462.
28. J.W.L. Yim, C.P. Grigoropoulos, Mismatched alloy nanowires for electronic structure tuning. J. Wu, Appl. Phys. Lett. 99 (2011) 233111-233113.
29. W. Shan, W. Walukiewicz, J. W. Ager, E. E. Haller, J. F. Geisz, D. J. Friedman, J. M. Olson, S. R. Kurtz, Band anticrossing in GaInNAs alloys. Phys. Rev. Lett. 82 (1999) 1221-1224.
30. H-J. Zhan, P-J. Zhou, Z-Y. He, Y. Tian, Microwave-assisted aqueous synthesis of small-sized, highly luminescent CdSeS/ZnS core/shell quantum dots for live cell imaging. Eur. J. Inorg. Chem. (2012) 2487-2493.

31. F. Aldeek, C. Mustin, L. Balan, G. Medjahdi, T. Roques-Carmes, P. Arnoux, R. Schneider, Enhanced photostability from CdSe(S)/ZnO core/shell quantum dots and their use in biolabeling. Eur. J. Inorg. Chem. (2011) 794-801.
32. D. Magde, R. Wong, P.G. Seybold, Fluorescence Quantum Yields and Their Relation to Lifetimes of Rhodamine 6G and Fluorescein in Nine Solvents: Improved Absolute Standards for Quantum Yields. Photochem. Photobiol. 75 (2002) 327-334.
33. B.C. Fitzmorris, J.K. Cooper, J. Edberg, S. Gul, J. Guo, J.Z. Zhang, Synthesis and Structural, Optical, and Dynamic Properties of Core/Shell/Shell CdSe/ZnSe/ZnS Quantum Dots. J. Phys. Chem. C 116 (2012) 25065-25073.
34. T. Fang, K. Ma, L. Ma, J. Bai, X. Li, H. Song, H. Guo, 3-Mercaptobutyric Acid as an Effective Capping Agent for Highly Luminescent CdTe Quantum Dots: New Insight into the Selection of Mercapto Acids. J. Phys. Chem. C 116 (2012) 12346-12352.
35. M. Geszke-Moritz, M. Moritz, Quantum dots as versatile probes in medical sciences: Synthesis, modification and properties. Mat. Sci. Eng C-Mater. 33 (2013) 1008-1021.
36. M.S. Neo, N. Venkatram, G.S. Li, W.S. Chin, W. Ji, Synthesis of PbS/CdS Core-Shell QDs and their Nonlinear Optical Properties. J. Phys. Chem. C 114 (2010) 18037-18044.
37. M. Booth, A.P. Brown, S.D. Evans, K. Critchley, Determining the concentration of CuInS2 quantum dots from the size-dependent molar extinction coefficient. Chem. Mater. 24 (2012) 2064-2070.

38. S.F. Wuister, F. van Driel, A. Meijerink, Luminescence and growth of CdTe quantum dots and clusters. Phys. Chem. Chem. Phys. 5 (2003) 1253-1258.

39. C. de Mello Donega´, S.G. Hickey, S.F. Wuister, D. Vanmaekelbergh, A. Meijerink, Single-step synthesis to control the photoluminescence quantum yield and size dispersion of CdSe nanocrystals. J. Phys. Chem. B 107 (2003) 489-496.

40. R.D Robinson, B. Sadtler, D.O. Demchenko, C.K. Erdonmez, L.W. Wang, A.P. Alivisatos. Spontaneous superlattice formation in nanorods through partial cation exchange. Science 317 (2007) 355–358.

41. J. Lee, H. Kim, S.J. Kahng, G. Kim, Y.W. Son, J. Ihm, H. Kato, Z.W. Wang, T. Okazaki, H. Shinohara, Y. Kuk, Bandgap modulation of carbon nanotubes by encapsulated metallofullerenes. Nature 415 (2002) 1005–1008.

42. J. Quyang, M. Vincent, D. Kingston, P. Descours, T. Boivineau, Md.B. Zaman, X. Wu, K. Yu, Noninjection, one-pot synthesis of photoluminescent colloidal homogeneously alloyed CdSeS quantum dots. J. Phys. Chem. C 113 (2009) 5193-5200.

43. B.O. Dabbousi, J. Rodriguez-Viego, V.F. Mikulec, J.R. Heine, H. Mattoussi, R. Ober, K.F. Jensen, M.G. Bawendi, (CdSe)ZnS core-shell quantum dots: synthesis and characterization of a size Series of highly luminescent nanocrystallites. J. Phys. Chem B 101 (1997) 9463-9475.

44. X. Wang, L. Qu, J. Zhang, X. Peng, M. Xiao, Surface-related emission in highly luminescent CdSe quantum dots. Nano Lett 3 (2003) 1103–1106.

45. M. Sanz, M.A. Correa-Duarte, L.M. Liz-Marzan, A. Douhal, Femtosecond dynamics of CdTe quantum dots in water. J. Photochem Photobiol A: Chem 196 (2008) 51-58.